Molecular Crystals and Liquid Crystals

Publication details, including instructions for authors and subscription information:
http://www.tandfonline.com/loi/gmcl20

APPLICATION OF POLYMER DISPERSED LIQUID CRYSTAL (PDLC) NEMATIC: OPTICAL-FIBER VARIABLE ATTENUATOR

H. Ramanitra [a], P. Chanclou [a], B. Vinouze [a] & L. Dupont [a]

[a] Ecole Nationale Supérieure des Télécommunications de Bretagne, Département d'Optique, Technopôle Brest-Iroise BP 832, 29285 Brest Cedex, France

Version of record first published: 15 Jul 2010

To cite this article: H. Ramanitra, P. Chanclou, B. Vinouze & L. Dupont (2003): APPLICATION OF POLYMER DISPERSED LIQUID CRYSTAL (PDLC) NEMATIC: OPTICAL-FIBER VARIABLE ATTENUATOR, Molecular Crystals and Liquid Crystals, 404:1, 57-73

To link to this article: http://dx.doi.org/10.1080/15421400390249952

Mol. Cryst. Liq. Cryst., Vol. 404, pp. 57–73, 2003

ISSN: 1542-1406 print/1563-5287 online
DOI: 10.1080/15421400390249952

Taylor & Francis
Taylor & Francis Group

APPLICATION OF POLYMER DISPERSED LIQUID CRYSTAL (PDLC) NEMATIC: OPTICAL-FIBER VARIABLE ATTENUATOR

H. Ramanitra, P. Chanclou, B. Vinouze and L. Dupont*
Ecole Nationale Supérieure des Télécommunications de Bretagne, Département d'Optique, Technopôle Brest-Iroise BP 832, 29285 Brest Cedex, France

Dispersions of liquid crystals in polymeric matrices (PDLC) are used as light Variable Optical Attenuators (VOAs). Electronically controllable VOAs play a crucial role for channel power equalizers in WDM systems. This article describes the theoretical model optimizing PDLC performance and the fabrication process utilizing the polymerization-induced phase separation (PIPS) method, and presents the optical attenuation (OA) and polarization dependence loss (PDL) characteristics versus fabrication conditions. Fabricated VOAs have a large attenuation range (10–30 dB) and low insertion loss (IL) at a 1.55 μm wavelength (0.5 dB). Depending on the fabrication parameters, the OA, IL, and PDL are optimized. This device needs an applied voltage V_{90} of 10 to 70 V_{rms} for 10–100 μm PDLC thickness. The flatness of the optical characteristics of this device has also been measured in the C + L band.

Keywords: liquid crystal nematic; electro-optic properties; polymerization; PDLC; VOA

INTRODUCTION

Liquid crystal (LC) materials are commonly used in displays, especially those with a twisted nematic structure. Polymer dispersed liquid crystals (PDLC) also use a nematic structure but in droplets inside the polymer; PDLC are used in reflective displays [1]. They consist of low molecular weight liquid crystals dispersed in a polymer matrix. Such materials possess electrically controllable optical properties, changing from a scattering composite in the absence of an electric field to a transparent composite upon its application [2]. Another application of such material

Received 26 February 2003; accepted 12 June 2003.
The author would like to thank all team of optical department ENST Bretagne LANNION for their helpful.
*Corresponding author. E-mail: hary.ramanitra@enst-bretagne.fr

is in the Variable Optical Attenuator (VOA). These are now playing an important role in optical communications for gain control of WDM networks and channel power equalization in WDM cross-connect nodes. Moreover, these components are used in channel blanking for network monitoring and signal attenuation for detector saturation protection [3]. Several techniques have been proposed for making VOAs, including mechanical attenuators having a large range of attenuation (>50 dB) but with low speed (∼1 s), high cost, and high bulk size which limit the applications. Waveguide-based VOAs have high-speed response (∼1 ms), but it is difficult to achieve a large attenuation range with low PDL [4]. Similarly, microelectromechanical system (MEMS) optical attenuators have a good dynamic range and better response times [5], but they too do not offer the desired features of a high-end VOA such as high dynamic range and fast switching speed. The VOA presented here is based on PDLC composite material. This technology has been applied to electrically controlled fibered VOAs in order to achieve high optical performance, compact size, low power consumption, and low cost. In the research reported here, we studied composite integration of a PDLC layer sandwiched between conductive coating optical fibers.

First, we give a brief physical description of the LC composite and present a theoretical analysis of light diffusion through PDLC composite. The physical properties of the LC nematic represent an essential parameter in the electro-optical operation of the PDLC composite. Second, we describe the electrode deposition, the polymerization process, and assembly. The key steps to achieving this VOA are attaching low-loss electrodes to the fibers and reducing the driving voltage. The coating process of the microlensed mode fiber is particular, due to the microoptic at the end of the single-mode fiber (SMF). The PDLC system is obtained by an irradiation ultra violet (UV) light polymerizing monomer. Before UV curing, fibers are inserted into the splicers and the gaps between the ends of each fiber are filled with an homogenous Monomer/LC solution. Finally, the evolution of the OA and PDL versus the UV power and the PDLC width are presented. In addition, we demonstrate the advantages and improvements that the expanded mode fibers can provide in comparison with SMFs and we give some characteristics (response time, flatness, ORL, etc.) of such a fabricated device.

PHYSICAL DESCRIPTION OF LC NEMATIC

If one considers the individual orientation of one LC molecule with respect to its neighbors, there are three main kinds of LC [6]: nematic, cholesteric, and smectic. We are interested here only in the nematic LC.

In the nematic phase, the molecules have an overall direction of orientation, but the positions of the individual molecules are still random. This orientational order allows an average direction of the molecules called the director to be defined, denoted by the vector $\vec{N}$. The material is still a fluid but at each point, **r**, in this fluid the molecules orient themselves along $\vec{N}(\mathbf{r})$: thus the material is anisotropic. Two different refraction indexes exist. The first index of refraction n_e corresponds to the index seen by a polarized light along the director of the liquid crystal. The other n_o is for light polarized perpendicular to the director. The optical anisotropy or birefringence is characterized by the difference between the extraordinary and the ordinary index: $\Delta n = n_e - n_o$. Nematics generally have a positive birefringence. We note that Δn depends on the wavelength and decreases with temperature until it becomes null in the isotrope phase.

The nematics present two dielectrics permittivity according to the axis. The dielectric constant parallel to the longitudinal axis of the molecule and the dielectric constant perpendicular to it are noted $\varepsilon_{\|}$ and $\varepsilon\perp$, respectively. The difference of the permittivity or dielectric anisotropy is defined by: $\Delta\varepsilon = \varepsilon_{\|} - \varepsilon\perp$. This property has an important consequence on aligning the director of LC when an external field electric field is applied because of the electrically induced dipolar moment. For a positive $\Delta\varepsilon$, molecules align themselves parallel to the electric field.

SCATTERING STATE MODEL FOR PDLC COMPOSITES

We recall that PDLC is composed of droplets of LC in a polymer matrix. The nematic directors $\vec{N}$of the droplets are randomly oriented. The light scattered by a PDLC is due to the refractive-index mismatch between the LC droplets and the polymer. There are different shapes of LC droplets such as spherical, ovoid, or convex. Depending on the fabrication conditions and the LC/polymer ratio, the droplets size varies from 10 nm to a few micrometers. The PDLC is quite an optically complex material. Besides the well-known Mie solution for scattering centers, there are several approximation approaches. The Rayleigh Gans Approximation (RGA) is suitable for small (compared to the wavelength) scattering centers and the Anomalous Diffraction Approach (ADA) [7] for large weakly refracting droplets. The ADA limit is reached when two conditions are found in the PDLC medium: $2\pi a/\lambda \gg 1$ and $m - 1 \ll 1$ (where a is the droplet sphere radius and m the relative refractive index of the scattering object) [8]. For small values of ka (when the droplet radius is close to the wavelength), the scattering cross section C_{sca}, defined by ADA, is given by

$$C_{sca} = 2\sigma_0(ka)^2[(n_{eff}(\theta)/np - 1)^2.\cos^2\alpha + (n_o/n_p - 1)^2.\sin^2\alpha] \qquad (1)$$

where $\sigma_0 = \pi a^2$, and n_p is the refractive index of the polymer, n_o is the ordinary index of the nematic LC, and $n_{eff}(\theta)$ is the effective refractive index meeting with the light scattering wave vector $\vec{k}$ when θ is the angle between $\vec{k}$ and $\vec{N}$ the nematic director of droplet. We introduce the polarization angle α between the electric field vector of the incident light and the plane defined by $\vec{k}$ and $\vec{N}$. We note that $(n_e(\theta)/n_p - 1)$ for PDLCs is less than 0.1, which validates the previous expression. Figure 1 illustrates the schematic representation of the scattering droplet and its projection on the plane perpendicular to the incident wave vector $\vec{k}$. In transmissive mode, after going through scattering sphere droplets, the transmitted light intensity, I_t, follows the Lamber-Beer law and can be expressed by

$$I_t = I_0 \, exp(-\chi.\langle C_{sca}\rangle.d) \tag{2}$$

where χ is the droplet concentration, d is the PDLC thickness, and I_0 is the incident light intensity. If we consider all angles, all the droplet C_{sca} contributions can then be added to calculate an average scattering coefficient in the wave vector direction. This means that, in the scattering state, the incident light beam meets with a random space distribution of $\vec{N}$ directors. Hence the scattering state C_{sca} can be expressed by

$$\langle C_{sca}\rangle = \frac{1}{2\pi}\int_0^{2\pi}\int_0^{\pi/2} C_{sca}(\theta,\alpha).\mathrm{Sin}\,\theta.\,d\theta.d\alpha \tag{3}$$

$\langle C_{sca}\rangle$ is introduced in the expression of I_t in Equation (2). Then, the optical attenuation OA is calculated using the following relation:

$$OA = 10\,Log_{10}(I_0/I_t) \tag{4}$$

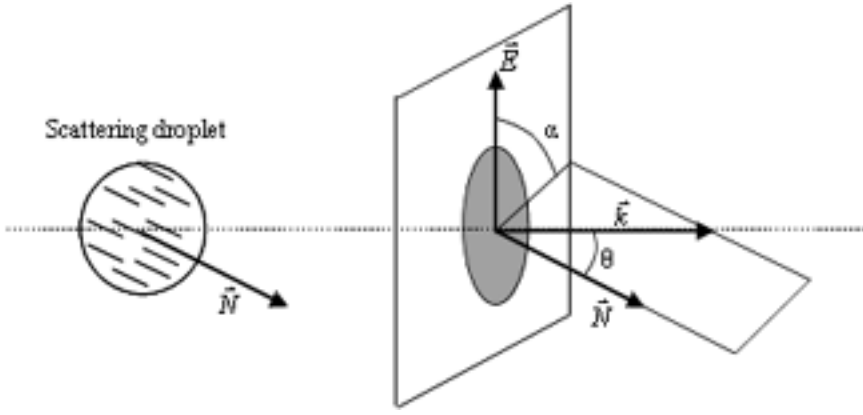

FIGURE 1 The projection of a scattering droplet on the plane perpendicular to the incident wave vector $\vec{k}$.

The OA depends on several parameters such as the droplets size a or the thickness d.

The general form of the equation governing the variation of the effective refractive index as a function of the applied voltage is given by

$$n_{eff}(V) = \eta + \kappa.\exp(-\mu.V^2) \tag{5}$$

where V is the applied voltage and η, κ, and μ are the constants. The effective refraction index evolution versus voltage is illustrated in Figure 2. In addition, we have the following three conditions allowing us to determine the three unknowns:

* $n_{eff} = n_{av} = \frac{n_e+2n_o}{3}$, where n_{av} is the average refraction index without applied voltage;
* $n_{eff}(\infty) = n_o$, when the molecules are aligned parallel to the electric field;
* $n_{eff}(V_{90}) = n_{eff}(\infty) + \frac{10}{100}.\left[n_{eff}(0) - n_{eff}(\infty)\right]$, corresponding to the saturation voltage V_{90}.

Thus, the final equation giving the effective refraction index can be expressed by

$$n_{eff}(V) = n_o + \frac{n_e - n_o}{3}.\exp\left[-\left(\frac{V}{V_{90}}\right)^2.\ln(10)\right] \tag{6}$$

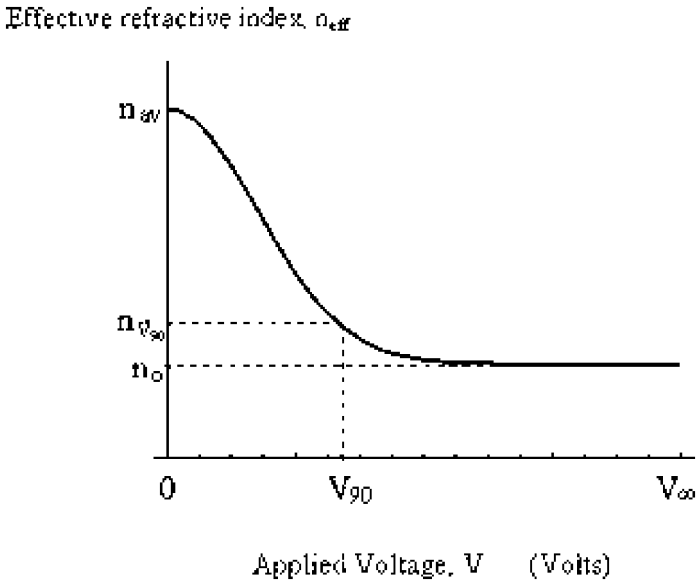

FIGURE 2 Evolution of the PDLC effective refractive index when voltage is applied.

This equation can be introduced in the relation in Equation (1) in order to obtain the transmitted intensity directly as a function of the applied voltage.

ELECTROOPTIC EFFECTS OF PDLC

We have used a new class of materials developed by Merck Ltd. (Germany) to realize the PDLC: a solution of monomer PN 393 with a refraction index n_p of 1.219, a low quantity of oligomer and UV photoinitiator, and a liquid crystal TL 205 ($\Delta n \approx 0.13$ at $\lambda = 1500\,nm$, $T = 20^\circ$ C) with a positive dielectric anisotropy ($\Delta\varepsilon = 5$ at 1 kHz and 20°C). The LC/monomer ratio for this mixture is about 80/20, which gives an isotropic solution at room temperature. After cell filling, this material is photopolymerized by UV light irradiation. The polymerization induces a phase separation, and the LC is rejected in droplets by the polymer. There are four phases for PDLC formation by UV-PIPS [9]. First, the monomer begins to polymerize when UV irradiation starts. After a short time, phase separation occurs between the growing polymer phase and the nematic phase and the solution bleaches. Phase separation goes on and shapes the polymer matrix until the time (around 100 to 200 s) when the PDLC structure is thoroughly fixed. We note that UV irradiation must be helped up to time "t_f" (final time) for complete monomer consumption in order to avoid short monomer molecules polluting the liquid nematic phase. The final time depends on the UV power and is reached when the energy level needed for the complete polymerization has been attained.

Light incident on this material is dispersed in the absence of an external alternating electric field because the principal optical axes of the droplets are randomly oriented in the polymer host. With application of the electric field, the long axes of the LC align themselves parallel to the field. Light now travels through the composite because the refractive index of droplets in the direction of the optical axis n_0 is chosen to be close to that of the polymer n_p [10]. Neither refraction nor scattering of the light will take place if the propagation direction is parallel to the electric field.

PDLC VOA

Figure 3 shows the functionality of a VOA using PDLC. The composite is inserted between the ends faces of two optical fibers [11] and adjusts their coupling efficiency. Here we utilize two types of fiber: single mode and microlensed. Fibers and PDLCs are self-aligned in a capillary. Without voltage, the nematic directors of the droplets are randomly oriented. The light crossing this PDLC composite is strongly scattered, so there is a low

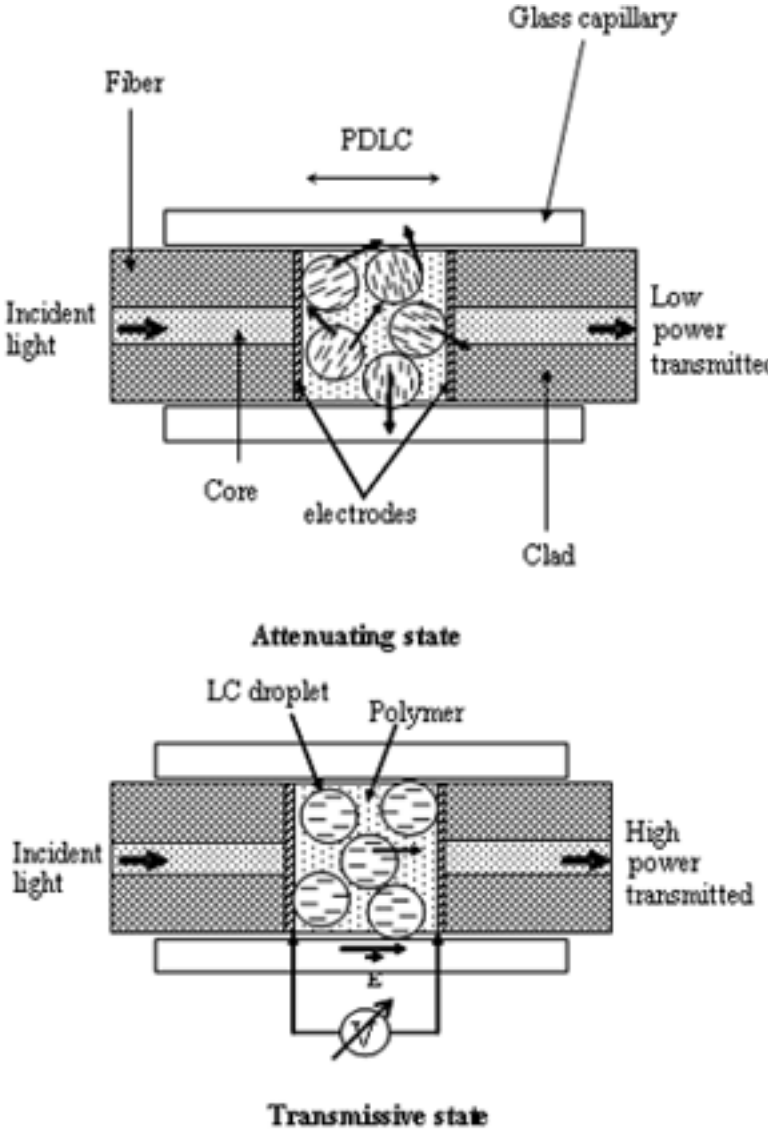

FIGURE 3 Principle of VOA optical functioning.

coupling efficiency between the input and the output fiber and the attenuation is maximum. When a voltage is applied across the composite, the LC molecules align themselves parallel to the electrical field and the material becomes transparent. So the coupling is maximum and the optical

attenuation is minimum. Between these extreme states, intermediate attenuations are controlled by intermediate voltages. Voltages are applied to the composite by using transparent electrodes deposited on the optical fibers [12].

VOA FABRICATION PROCESS

In this research, we utilize two types of optical fiber as shown in Figure 4. The first one corresponds to a standard SMF with a spot size $2\omega_0 = 10.5 \pm 1\,\mu m$ at wavelength $\lambda = 1.55\,\mu m$ (determined at $1/e^2$ of the maximum intensity) and the Fresnel length is given by the relation: $L_F = K_0.\omega_0^2/2\pi$, where k_0 is the propagation constant with $k_0 = 2\pi/\lambda$. This theoretical value is then estimated at about 18 μm. The second corresponds

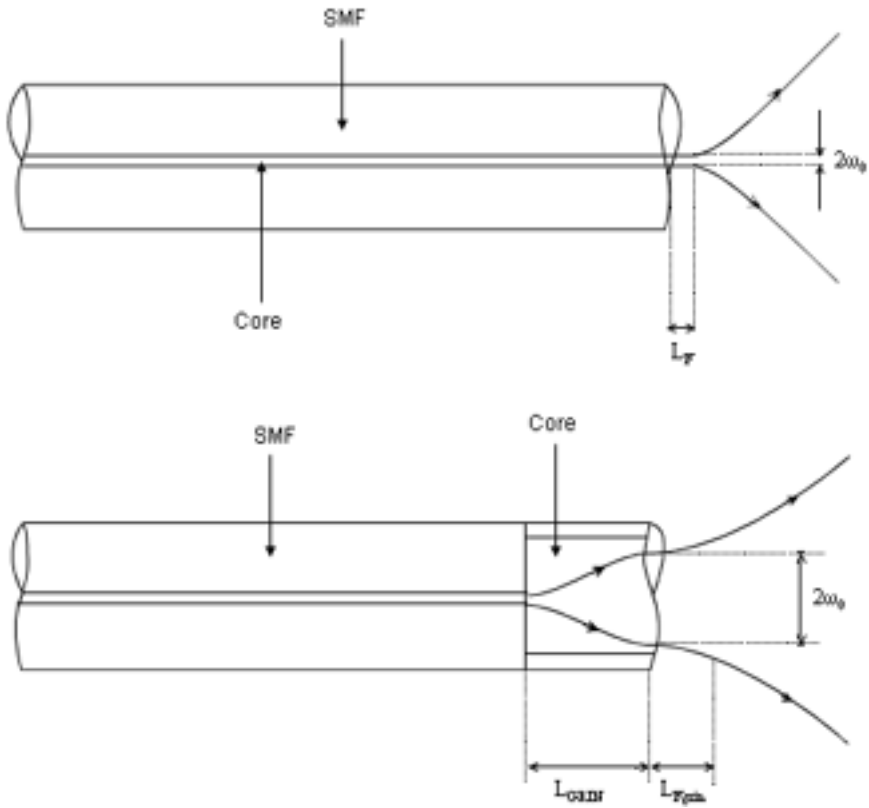

FIGURE 4 Beam propagation in the SMF and microlensed SMF ends.

to a microlensed SMF. This fiber is composed of a graded index (GRIN) section spliced to the end face of the SMF (see Figure 4). The GRIN section length L_{GRIN} is optimized at 370 μm to reach around 28 ± 1 μm of the mode diameter and about 126 μm of the GRIN Fresnel length L_{Fgrin} [13–15]. Therefore, the main advantage of this arrangement compared to a standard SMF involves multiplying by 3 the spot diameter and so facilitate the coupling between the two fibers.

In order to apply a voltage across the composite, the fibers are metallized by Au-Pd via a sputtering process. A highly conductive coating is deposited on the periphery of the fiber and, after cleaving, a transparent electrode is deposited on the cleaved face. The transparent electrode has 93% transmittance and this thickness is estimated between 20 and 50 nanometers. The metallization process of the microlensed SMF is different from that of the standard SMF because the multimode step index fiber section spliced to the end of the SMF must not be cleaved. Before the thick conductive layer, we depose a resin layer at the output of the microlensed SMF. After electrode deposition, the resin is then stripped. Figure 5 details the metallization process of the microlensed SMF using resin to avoid cleaving the GRIN section. The end faces of the coated SMF or the coated

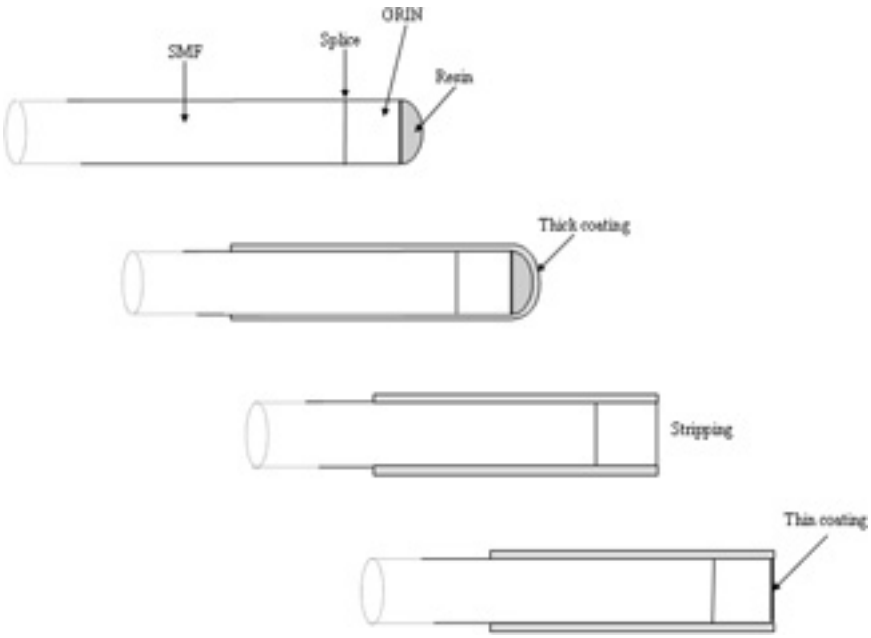

FIGURE 5 The different steps of microlensed fiber's metallization process.

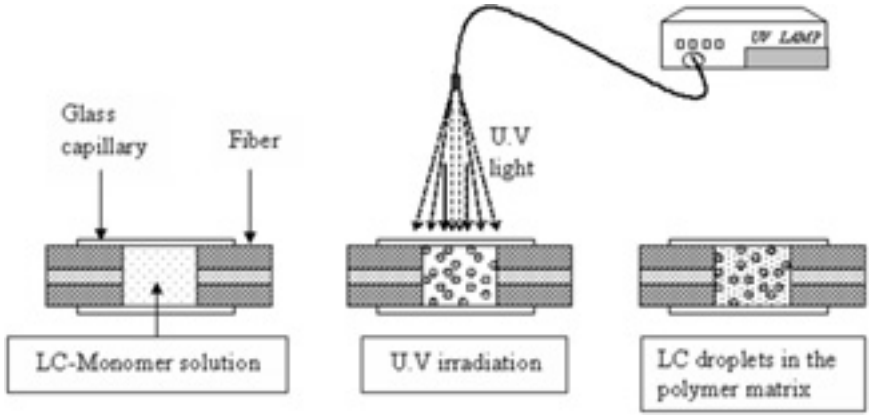

FIGURE 6 PDLC formation by U.V-PIPS process.

microlensed SMF have an excess loss of about 0.2 dB. We used glass microcapillary with a 126 μm internal diameter, in which a LC-monomer mixture was previously filled. After coating, the two fibers are inserted into each end of the glass capillary (see Figure 7(a)). A gap of 10–100 μm is adjusted between the fiber end faces.

The mixture is then U.V polymerized in the next step. We choose the case of PIPS, by means of an UV light polymerizing monomer as shown in Figure 6. The UV light is provided by a medium pressure mercury lamp already implemented with an UV filter to avoid short wavelengths (<300 nm). This process appears very important for the device's

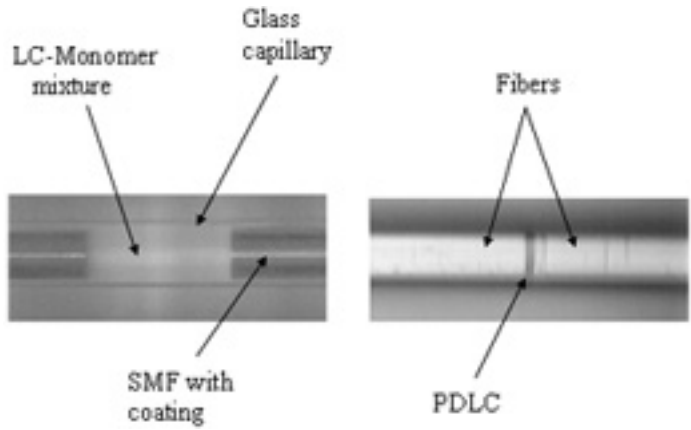

FIGURE 7 (a) Microscopic view during introduction of fibers; (b) Microscopic view of the VOA after polymerization (PDLC thickness 50 μm).

characteristics because the LC droplet size of the PDLC depends on the UV power. Moreover, UV energy plays an important role to end chemical reactions after the phase separation. In our case, VOAs were polymerized by a UV energy minimum of 10 J/cm^2 for complete monomer consumption and to stabilize the electro-optical properties of the PDLC in the course of time. Figures 7(a) and 7(b) give a view of the device during this process and after polymerization.

EXPERIMENTAL RESULTS AND DISCUSSION

This paragraph presents the performances of our VOA device according to the fabrication conditions. Experimentally, we made several $50 \pm 5\,\mu m$ gap VOAs using standard SMFs. Figure 8 shows the OA range and PDL versus UV power. The curve presents an OA range optimum of about 28 dB obtained at 25 mW/cm^2, but a large value of PDL (11 dB) was measured in this optimum. The PDL decreases with increasing UV power and the device attains its minimum value of PDL (1.8 dB) at 150 mW/cm^2. This means that the large number of droplets involves a strong random phenomenon on polarization. In this case, the diffuser centers become too small and the OA range falls. With high UV irradiation, the OA range decreases slowly because the evolution of droplet size becomes almost stable in relation to the UV light. In this work, we utilize higher UV power in comparison with a standard PDLC cell [6] because the LC-monomer mixture in the optical path cannot receive complete UV power due to the trenches ($\sim 60\,\mu m$) of parasite PDLC.

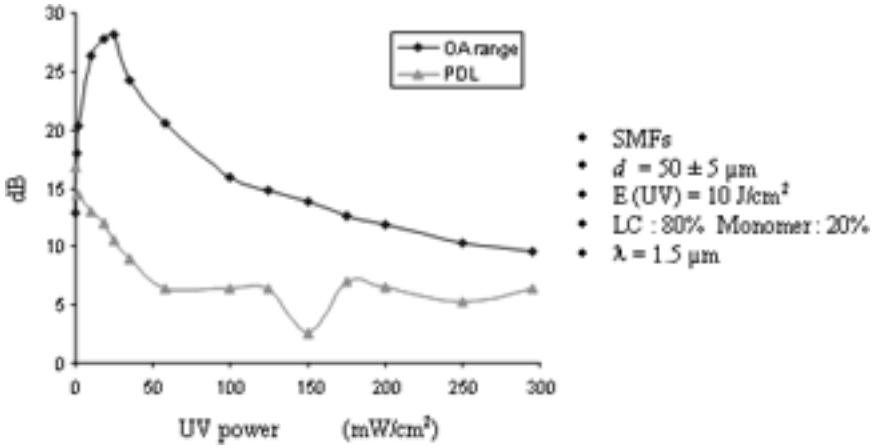

FIGURE 8 Optical characteristics of the PDLC VOAs versus U.V power.

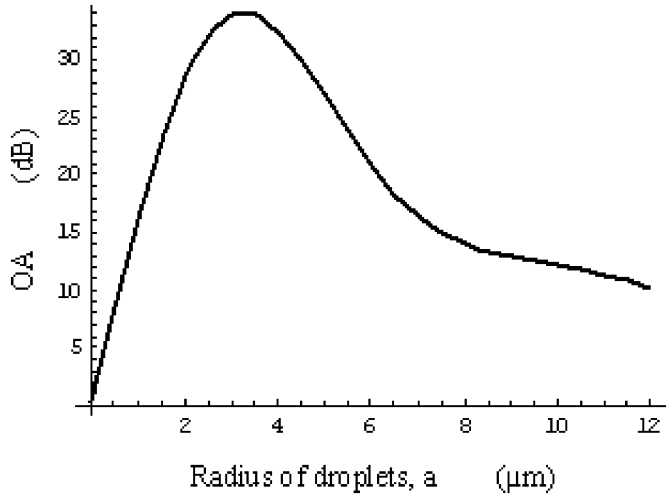

FIGURE 9 Simulation of OA versus droplet LC radius according to ADA for a 45 μm of PDLC thickness.

Figure 9 shows the calculated OA at $\lambda = 1.55\,\mu m$ versus the droplet radius, according to ADA. This curve shows the possibility of obtaining a very large attenuation (around 30 dB) when the PDLC droplet size reaches around 3.3 μm. In the scattering state, there is an optimum of radius where the attenuation is maximal [4]. The expression

$$a_{opt} = \frac{0.3}{\Delta n}.\lambda \tag{5}$$

gives its theoretical value, estimated at 3.5 μm. As the UV radiation has a direct influence on droplet radius (the higher the UV power, the smaller the droplets), the experimental curve follows the same behavior as the theoretical estimation with an OA range optimum obtained at 25 mW/cm^2 corresponding to a droplet radius of about 3.5 μm.

The experimental points and theoretical curve (for droplet radius $a = 0.75\,\mu m$) of OA versus composite thickness "d" cured at 150 mW/cm^2 are shown in Figure 10. The OA achieves 28 dB for a 100 μm gap, and its behavior follows a linear variation as predicted by the Beer-Lambert law. For the same droplet size, the incident light becomes highly scattered if the PDLC thickness increases as demonstrated in the relation in Equation (2). Moreover, the PDL increases with the OA and achieves 15 dB at a gap of 100 μm as demonstrated in Figure 11, showing an addition of droplet directors. In fact, the UV irradiation direction induces a quasi-privileged direction of LC directors in the droplets and this phenomenon is accentuated when the number of LC droplets increases. We measured a

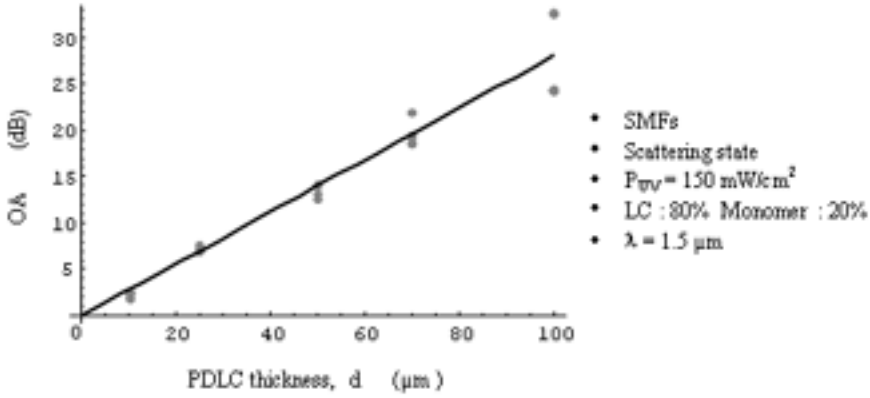

FIGURE 10 Experimental points and theoretical curve of OA's VOA with several PDLC gaps.

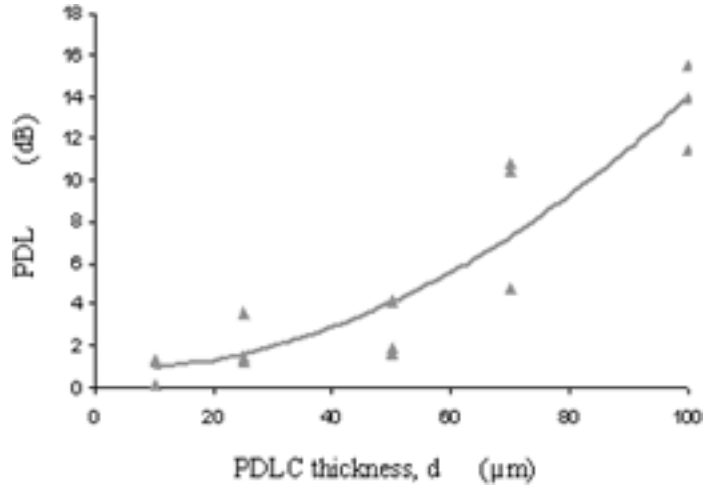

FIGURE 11 The approximate curve and experimental points of the PDL versus PDLC gaps.

large IL (2.5 dB) and a high driving voltage (around 100 V_{rms}) at this gap width.

Figure 12 shows the simulation and the experimental measurements of the electro-optic effect corresponding to VOAs using standard SMFs and microlensed SMFs. The device was cured under UV irradiation at 150 mW/cm^2, where the PDL is minimal, for an identical gap of 50 μm. These curves demonstrate that OA is greater with microlensed fibers (17.5 dB) compared with the OA of the VOAs using SMFs (13.9 dB). When the spot size is

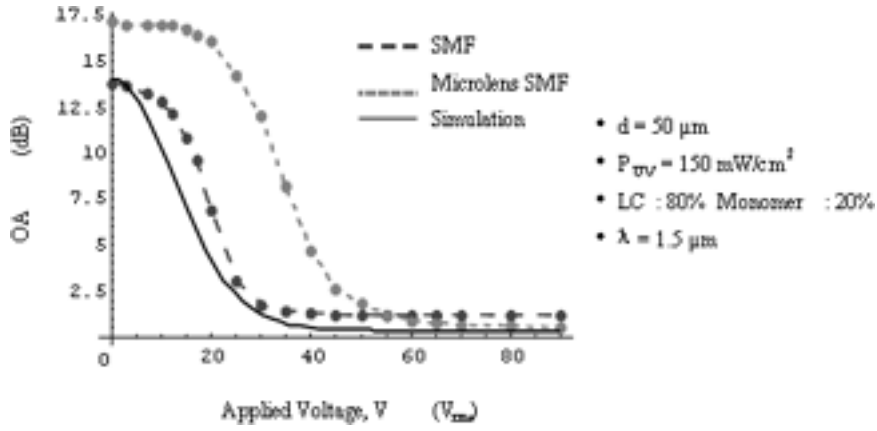

FIGURE 12 Simulation and typical OA of the VOA with SMF and microlensed SMF.

expanded and the number of diffuser centers in the optical path increases, the multiple diffusion phenomenon (not detailed here) appears to imply a rise in OA. The IL of about 0.5 dB (instead of 1.2 dB for the SMF) is considered to be the sum of the thin coating on the ends of the fibers (0.2 dB*2), and 0.1 dB due to the PDLC absorption and a low misalignment lateral on fiber coupling. The large working distance of the microlensed fiber involves wide misalignment tolerances to achieve a device with a low coupling loss. The experimental value of the IL is higher in comparison with the calculated value (0.3 dB) due to metallization and the fiber coupling losses. But, the experimental values of the threshold voltage V_{10} (15 V_{rms}) and the saturation voltage V_{90} (50 V_{rms}) increase slightly due to the process of coating. Voltage driving with VOA of the standard SMF is estimated to be about 0.7 V per µm of PDLC composite. The simulation gives a very low threshold voltage (around 5 V_{rms}) because the anchorage strength of the LC molecules in contact with the polymer is not considered in the theoretical model. We note a good similarity between the simulation and the experimental results of the SMF's VOA.

PDL behavior with their two types of VOA is compared in Figure 13. We note that the PDL is only about 1.8 dB for the SMF, whereas that of the microlens fiber rises to 3.2 dB. This result can be interpreted by the phenomenon of the quasi-privileged direction of LC molecules coming from UV irradiation, and this effect is also accentuated when more LC droplets are lighted with a larger incident beam. Additionally, not all the trenches of PDLC can receive the same UV power, and this means a gradient of droplet size [16]. So, the molecules with a smaller droplet size are faster than the molecules with a larger droplet size under an electric field. The PDL

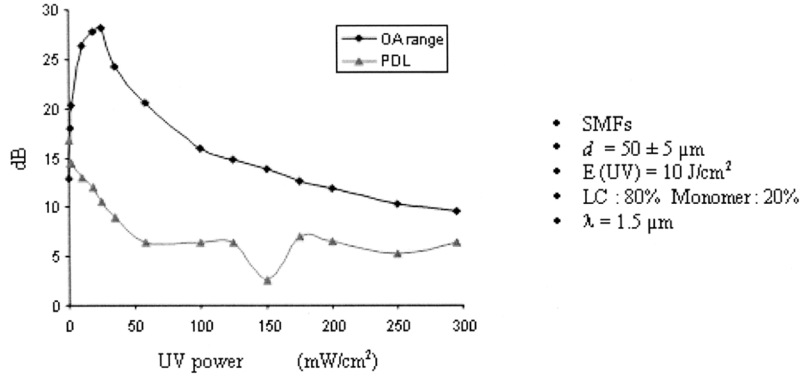

FIGURE 13 Typical PDL property of the VOA with SMF and microlensed fiber.

increases slowly up to the threshold voltage and decreases to become practically null at the saturation voltage. In fact, this effect increases around the threshold voltage (perfect privileged direction of LC) before the LC molecules align themselves completely with the electric field.

Figure 14 illustrates the wavelength dependence of the OA range and the PDL for an SMF VOA. In the C + L wavelength range the attenuation flatness is below 1.5 dB, whereas the PDL flatness is around 0.3 dB. This performance appears very important because the VOA will be placed in a WDM transmission line using many wavelengths in the C + L band. For our

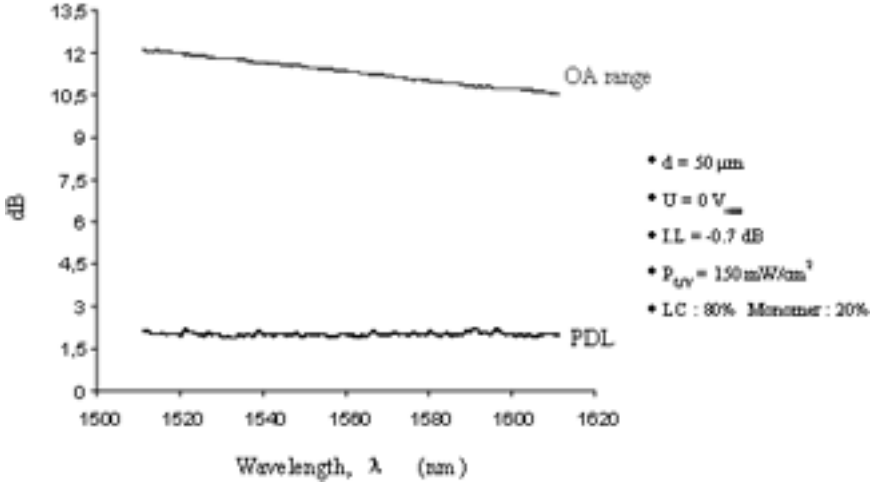

FIGURE 14 The wavelength dependence of VOA's properties in the C+L range.

VOA fabrication, we used standard fibers cleaved on the slant (about 8° angle) in order to improve the optical return loss (ORL). The value maximum of the ORL obtained in the C + L band is around −37 dB. This parameter is primordial in telecom networks because a high reflection light involves destruction of the laser transmitter.

CONCLUSION

This article describes a compact fibered VOA using a PDLC in a capillary. The fabrication process of the attenuator requires simple steps and is particularly suitable for low-cost systems. With PDLC, the fabrication problems inherent to other types of LC are not encountered. This simplifies the design and increases reliability, making it particularly suitable for optical communication applications. The OA range can be optimized by varying the UV curing power, by increasing PDLC thickness, or by using microlensed mode fibers to fabricate our device. For a typical gap of 50 μm, the insertion loss is low (<1 dB) and the attenuation range reaches around 30 dB with a driving voltage of 35 Vrms. The VOA's estimated power consumption is very low (<1 μW), and response times of a few ms can be obtained in the PDLC composite. The polarization dependence is <1.8 dB for the device using standard SMF and <3.2 dB for the device with microlensed SMF, whereas a flatness of 1 dB and −37 dB of ORL max were measured in the C + L band. Unfortunately, the PDL value is still too high for telecommunications specifications (PDL <0.5 dB). Their optical performance could be improved by optimizing polymerization conditions, for example by directly injecting the UV beam into the optical fiber.

REFERENCES

[1] Vinouze, B., Bosc, D., Guilbert, M., & Trubert, C. (1994). Active matrix with optimised PDLC for reflective direct view liquid crystal display. In: *IDRC Proceedings 1994*, IDRC, Monterey, CA, 472–475.

[2] Stein, R. S., & Srinivasarao, M. (1993). Light scattering of liquid crystal dispersions. *SPIE, 1911*, 132–149.

[3] Hirabayaschi, K., Wada, M., & Amano, C. (2001). Compact optical-fiber variable attenuator arrays with polymer-network liquid crystals. *Applied Optics*, *40*, 3509–3517.

[4] Lee, S.-S., Jin, Y.-S., Son, Y.-S., & Yoo, T.-K. (1999). Polymeric tunable optical attenuator with an optical monitoring tap for WDM transmission network. *IEEE PhotonTechnol. Lett.*, *11*, 590–592.

[5] Giles, C. R., Aksyuk, V., Barber, B., Ruel, R., Stulz, L., & Bishop, D. (2001). A silicon MEMS optical switch attenuator and its use in lightwave subsystems. *IEEE J. Select. Topic. Quantum Elect.*, 5, 18–25.

[6] Bahadur, B. (1990). *Liquid Crystals—Applications and Uses.* World Scientific Publishing Co. Pte. Ltd. Vol. 1, pp. 140–169.

[7] Zumer, S. (1988). Light scattering from nematic droplets: anomalous diffraction approach. *Physical Review A*, *37*, 4006.
[8] Bosc, D., Trubert, C., Vinouze, B., & Guilbert, M. (1996). Validation of a scattering state model for liquid crystal polymer composites. *Appl. Phys. Lett.*, *68*, 2489–2490.
[9] Bosc, D., Guilbert, M., Trubert, C., & Vinouze, B. (1996). Improvements in fabrication conditions of Liquid Crystal-Polymer Composite Cells. *Mol. Cryst. Liq. Cryst.*, *287*, 83–92.
[10] Lacquet, B. M., Swart, P. L., & Spammer, S. J. (1997). Polymer dispersed liquid crystal. Fiber optic electric field probe. *IEEE Transactions on Instrumentation and Measurement*, *46*, 31–35
[11] Philip, B., Michael, J., Friedrich, S., & Scott, R. (1991). Liquid crystal fiber optic attenuator and process for making same. Techtronix INC (US). US Patent 5015057.
[12] Hirabayaschi, K., Wada, M., & Amano, C. (2001). Optical-fiber variable-attenuator arrays using polymer-network liquid crystal. *IEEE Photonics Technology Letters*, *13*, 487–489.
[13] Einkey, W. L., & Jack, C. A. (1987). Analysis and evaluation of graded-index fiber-lenses. *J. Lightwave Technol.*, *LT-5*, 1156–1164.
[14] Shiraishi, K., Aizawa, Y., & Kawakami, S. (1990). Beam expanding fiber using thermal diffusion of the dopant. *J. Lightwave Technol.*, *8*, 1151–1161.
[15] Chanclou, P., Ramanitra, H., Gravey, P., & Thual, M. (2002). Design and performance of expanded mode fiber using microoptics. *J. Lightwave Technol.*, *20*, 808–814.
[16] Lucchetta, D. E., Francescangeli, O. F., Lucchetti, L., Gobbi, L., & Simoni, F. (2001). Morphological and electro-optical properties of polymer dispersed liquid crystals cured by high intensity laser radiation. *Mol. Cryst. Liq. Cryst.*, *367*, 313–321.